Tenth U.S. National Conference on Earthquake Engineering
Frontiers of Earthquake Engineering
July 21-25, 2014
Anchorage, Alaska

PRELIMINARY RESULTS FOR NEESR FULL-SCALE RC COLUMN TESTS UNDER COLLAPSE-CONSISTENT LOADING PROTOCOLS

A. Nojavan[1], A.E. Schultz[2], S-H. Chao[3], C. Haselton[4], S. Simasathien[5], G. Palacios[5], and X. Liu[6]

ABSTRACT

Direct collapse simulation is a critical tool for understanding the behavior of reinforced concrete (RC) buildings subjected to extreme earthquakes. However, there are major shortcomings in currently available test data for modern RC moment frame columns in order to develop suitable models for the collapse simulation. Most of the currently available test data correspond to smaller scale specimens subjected to deformation levels that are not large enough to capture accurately their degradation and softening behavior. Moreover, there are limited test data available for identical specimens tested under monotonic and cyclic loading protocols. To address this critical need, a set of full-scale reinforced concrete columns was tested at the NEES (Network for Earthquake Engineering Simulation) Multi-Axial Sub-assemblage testing (MAST) facility at the University of Minnesota as part of a U.S. National Science Foundation (NSF) NEES research project. The specimens had cross sectional dimensions that were larger than most if not all columns tested previously under simulated seismic loading. The specimens were subjected to large monotonic and cyclic displacement reversals up to 10% story drift ratio to investigate the behavior at or near collapse conditions. An overview of the load-deformation relations, strength and stiffness deterioration, and the effect of loading protocols are discussed.

[1]Graduate Research Assistant, Dept. of Civil Engineering, University of Minnesota, nojav002@umn.edu
[2]Professor, Dept. of Civil Engineering, University of Minnesota, Minneapolis, MN55455, schul088@umn.edu
[3]Associate Professor, Dept. of Civil Engineering, University of Texas at Arlington, Arlington, TX 76019
[4]Associate Professor, Dept. of Civil Engineering, California State University, Chico, CA 95929
[5]Graduate Research Assistant, University of Texas at Arlington, Arlington, TX 76019
[6]Former Post-doctoral Research Fellow, University of Texas at Arlington, Arlington, TX 76019

Nojavan A, Schultz AE, Chao S-H, Haselton C, Simasathien S, Palacios G, and Liu X. Preliminary results of NEESR full-scale RC columns subjected to collapse-consistent loading protocols for enhanced collapse simulation. *Proceedings of the 10th National Conference in Earthquake Engineering,* Earthquake Engineering Research Institute, Anchorage, AK, 2014.

DOI: 10.4231/D3C824F6F

Tenth U.S. National Conference on Earthquake Engineering
Frontiers of Earthquake Engineering
July 21-25, 2014
Anchorage, Alaska

Preliminary Results for NEESR Full-Scale RC Column Tests under Collapse-Consistent Loading Protocols

A. Nojavan[1], A.E. Schultz[2], S-H. Chao[3] , C. Haselton[4] , S. Simasathien[5], G. Palacios[5], and X. Liu[6]

ABSTRACT

Direct collapse simulation is a critical tool for understanding the behavior of reinforced concrete (RC) buildings subjected to extreme earthquakes. However, there are major shortcomings in currently available test data for modern RC moment frame columns in order to develop suitable models for the collapse simulation. Most of the currently available test data correspond to smaller scale specimens subjected to deformation levels that are not large enough to capture accurately their degradation and softening behavior. Moreover, there are limited test data available for identical specimens tested under monotonic and cyclic loading protocols. To address this critical need, a set of full-scale reinforced concrete columns was tested at the NEES (Network for Earthquake Engineering Simulation) Multi-Axial Sub-assemblage testing (MAST) facility at the University of Minnesota as part of a U.S. National Science Foundation (NSF) NEES research project. The specimens had cross sectional dimensions that were larger than most if not all columns tested previously under simulated seismic loading. The specimens were subjected to large monotonic and cyclic displacement reversals up to 10% story drift ratio to investigate the behavior at or near collapse conditions. An overview of the load-deformation relations, strength and stiffness deterioration, and the effect of loading protocols are discussed.

Introduction

Development of improved component models that are capable of capturing and predicting collapse of structural systems more accurately is among the top research priorities of the recent National Institute of Standards and Technology (NIST) and National Earthquake Hazards Reduction Program (NEHRP) reports [1, 2]. These component models are required for defining collapse-safety limit states in the implementation of the next generation of performance-based seismic design procedures [3, 4]. To develop such analytical models for reinforced concrete (RC) columns, an enhanced understanding of their behavior when subjected to extreme loading conditions is critically important. To attain such understanding, much research has been focused

[1]Graduate Research Assistant, Dept. of Civil Engineering, University of Minnesota, nojav002@umn.edu
[2]Professor, Dept. of Civil Engineering, University of Minnesota, Minneapolis, MN55455, schul088@umn.edu
[3]Associate Professor, Dept. of Civil Engineering, University of Texas at Arlington, Arlington, TX 76019
[4]Associate Professor, Dept. of Civil Engineering, California State University, Chico, CA 95929
[5]Graduate Research Assistant, University of Texas at Arlington, Arlington, TX 76019
[6]Former Post-doctoral Research Fellow, University of Texas at Arlington, Arlington, TX 76019

Nojavan A, Schultz AE, Chao S-H, Haselton C, Simasathien S, Palacios G, and Liu X. Preliminary results of NEESR full-scale RC columns subjected to collapse-consistent loading protocols for enhanced collapse simulation. *Proceedings of the 10th National Conference in Earthquake Engineering,* Earthquake Engineering Research Institute, Anchorage, AK, 2014.

on experimental behavior of reinforced concrete columns. Properties of more than 300 tests on rectangular RC columns is included in the PEER structural performance database [5], however almost all of the current test data are related to columns with cross-sectional dimensions no larger than 24×24 in. yet in practice, typical columns in seismic regions of the US can be considerably larger. Also, most of the currently available test data correspond to specimens subjected to deformation levels that are not large enough to capture their degradation and softening behavior accurately [5, 6, 7, 8]. Moreover, there are limited test data available for identical specimens tested under various loading protocols [9, 10].

Previous research has clearly shown that loading history has an important effect on the behavior of RC members [9, 11, 12, 13, 14]. In many of these experimental research efforts, RC columns have been subjected to either a constant [15, 16, 17] or variable [18, 19] axial load along with symmetric displacement reversals. However, columns in an actual building frame will be exposed to non-symmetrical displacement excursions during earthquakes. Therefore, it is of interest to assess the behavior of RC columns under non-symmetrical cyclic loading protocols as well. In addition, even symmetric loading protocols can include many different features associated with the manner in which peak drift for each cycle evolves during the protocol.

This research aims to enhance understanding of the behavior of RC columns when subjected to near-collapse loading protocols. To this end, the experimental program addresses the shortcomings of the available test data for RC columns. The specimens featured two different cross-sectional dimensions (36×28 in. and 28×28 in) that are larger than most if not all columns tested previously under simulated seismic loading. The specimens were subjected to large monotonic and several cyclic loading protocols. The loading protocols simulated essential features of seismic loading at the near-collapse state, at which story drift ratios were approaching 10%, and under which the columns lost most of their strength and exhibited highly nonlinear behavior.

Experimental Program

Seven full-scale RC columns that featured different cross-sectional dimensions were built and tested under distinct axial load ratios, and various lateral loading protocols. The lateral loading was applied as displacement cycles along the SE-NW faces of the column specimens for uniaxial tests (Fig. 1) and along two perpendicular directions for the biaxial test. All the specimens were constructed and cast in an upright position at the University of Texas at Arlington, and they were tested at the Multi-Axial Sub-assemblage Testing (MAST) lab of the University of Minnesota. The 6-degree-of-freedom (6-DOF) loading system at the MAST lab is capable of applying up to 1,320 kips of vertical force, 880 kips of lateral force in the orthogonal directions with strokes of ±16 in., and 8,910 kip-ft of moments [20].

Specimens

The specimens in the experimental program are representative of a portion of a column bent in a double-curvature at the ground floor of a prototype 20-story high-rise building. The specimen

represents that portion of the column that spans from the base to a location above the inflection point but below the top of the column. The columns were designed according to seismic provisions in Chapter 21 of ACI 318-11 [21], and were constructed with two different cross-sectional dimensions designated as Perimeter-Frame (PF) which represents more recent RC moment frames, and is used in combination with post-tensioned flat slab gravity systems; and Space-Frame (SF) which represents widely used moment frames in the past decades. The former is an interior column along perimeter frames which primarily resist lateral forces, whereas the latter is an interior column in a space frame which carries both lateral and gravity loads. The PF specimens were constructed with sixteen (16) #9 longitudinal bars, and had a cross-sectional dimension of 36×28 in., whereas twelve (12) #8 longitudinal bars were used in the SF columns with 28×28 in. cross section as shown on Fig.1. Longitudinal bars were tied with #5 hoops placed with 5 or 6 in. spacing depending on their distance from the column base. All specimens were 106 in. in height, and were cast along with an 84×84×30 in. footing block and a 75×75×23 in. loading block. The footing block connects to a post-tensioned, three-piece base block of 102×102×60 in. dimensions which itself is attached to the lab strong floor using 1½ in. ASTM A193 Grade B7 threaded rods with a minimum yield strength of 125 ksi. The loading block connects to the loading frame crosshead using the same threaded rods. The whole testing specimen had a height of 219 in. under the loading crosshead.

Reinforcing steel and concrete

Longitudinal reinforcement were either No. 8 bars (specimens CII-2), or No. 9 bars (all others) ASTM A706 Grade 60, whereas transverse hoops were No. 5, ASTM A615 Grade 60. Uniaxial tensile tests were conducted on steel coupons according to ASTM A370-03a [22] to measure mechanical properties of steel bars using a 200-kip universal testing machine with hydraulic grips. In addition to the applied force and displacement, strains were captured by an extensometer located at mid-length of each sample. Measured values of yield strength (f_y), ultimate strength (f_u), calculated yield strain (ε_y), and measured ultimate strain (ε_u) are given in Table 1.

The concrete used in the specimens was nearly self-compacting with maximum aggregate size of 3/8 in., and the specified nominal 28-day strength of 5000 psi. The concrete strength of each specimen was determined by standard cylinder tests according to ASTM C39C [23]. For each specimen, three 4×8 in. cylinders were tested at the specimen testing day. Average measured compressive strengths at the testing day for specimens are presented in Table 1.

Instrumentation

Specimens were instrumented to measure deflection, rotation, and strains at several portions of the specimens. DC-operated linear variable deflection transformers (LVDTs) were installed vertically on opposite faces of the specimens to measure curvature along the height. Additional horizontal LVDTs were used to measure horizontal deflection. String potentiometers were installed diagonally to record shear deformations. Transverse displacement of the specimens at the inflection point was recorded using string potentiometers. An inclinometer was also installed at the inflection point to capture rotations, and strain gages were used to measure longitudinal and transverse steel and concrete core strains at discrete locations along column height and

within the cross section.

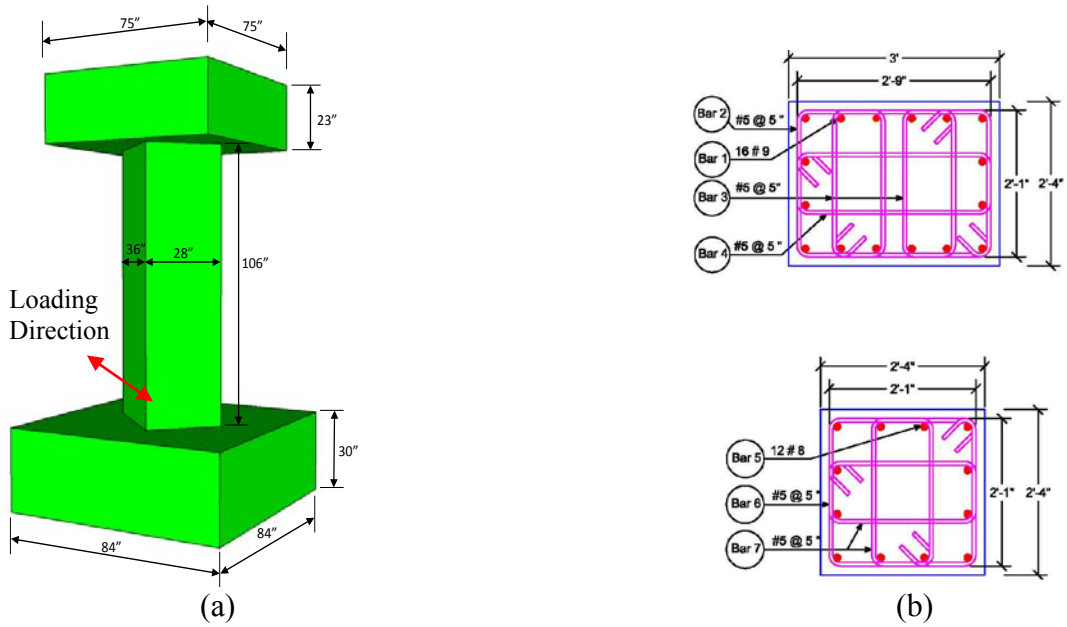

Figure 1. Column specimen assembly and detailing: (a) 3D rendering of PF specimens, (b) cross-sectional detailing of PF (top) and SF specimens (bottom).

Table1. Material properties of the specimens.

Sp.	$b \times h$ (in.)	f'_c (psi)	age (days)	Longitudinal Reinforcement					Transverse Reinforcement				
				Bar Size	f_y (ksi)	f_u (ksi)	ε_y	ε_u	Bar Size	f_y (ksi)	f_u (ksi)	ε_y	ε_u
CI-4	36×28	4,860	28	9	74	112	0.0025	0.2	5	69	104	0.0022	0.12
CI-2	36×28	5,400	28	9	74	112	0.0025	0.2	5	66	108	0.0023	0.12
CI-5	36×28	5,300	28	9	74	112	0.0025	0.2	5	65	105	0.0022	0.12
CI-6	36×28	5,370	20	9	74	112	0.0025	0.2	5	65	105	0.0022	0.12
CII-2	28×28	5,270	21	8	59	102	0.002	0.15	5	64	103	0.0022	0.12
CI-1	36×28	4,610	19	9	74	112	0.0025	0.2	5	65	105	0.0022	0.12
CI-7	36×28	4,900	14	9	74	112	0.0025	0.2	5	62	103	0.0021	0.11

Loading Protocols

To assess the effect of loading protocols on the behavior of specimens, six loading protocols were designed and used during the tests. An axial load was applied at the beginning of each test and kept constant during the test. The axial load ratio P/P_0 was 0.15 and 0.3 for perimeter frame, and space frame columns, respectively; where P_0 is the gross cross-sectional axial capacity for the concrete ($P_0 = f'_c A_g$) and A_g is the gross cross-sectional area of each specimen. These axial load ratios are representative of columns in a typical 20-story building experience in practice: a large axial load ratio makes the behavior less ductile, while specimens approach pure flexural behavior under small axial load ratios. Specimens were then subjected to displacement reversals until a stopping criterion for the test was satisfied. Stopping criteria were needed so that the test could go as far into the load degradation region as possible without risking the safety of the

equipment and users. There were two criteria for stopping the tests:

1) When specimens lost significant strengths (i.e. the residual strengths dropped to 20% of their peak capacities)
2) When hydraulic actuators reached their maximum stroke angle

In the case of the second condition, loading could still continue in the opposite direction if desired. The loading protocols that were applied to the specimens are illustrated in Fig. 2.

The first specimen (CI-4) was subjected to Loading Protocol 4 in which a monotonic displacement was applied in one direction until the actuators reached their maximum stroke angle at about 15½ in. of lateral displacement at the crosshead. Loading was then similarly continued in the opposite direction, and then back to zero displacement. The idea behind this protocol was to reach the 10% drift ratio limit in one direction, and then to do the same in the other direction. So, strictly speaking the loading protocol 4 is a hybrid protocol, that is, a pseudo-monotonic cycle. Loading protocol 4 was designed to illustrate the strength and displacement capacity of the specimens, and was helpful in designing a control scheme for the rest of the specimens.

RC columns in an actual building will typically experience many small cycles before the main shock by an earthquake; therefore, a cyclic loading protocol is a more appropriate loading scheme that structures will experience in practice. ACI 374-05 provides standard guidelines for designing displacement controlled cyclic loading schemes that are representative of the applied loads in a seismic excitation. Therefore, except the monotonic, and a near-collapse loading protocols, all other specimens were subjected to cyclic loading based, in part, on ACI 374-05. In the Loading Protocol 2, the specimens (CI-2, CII-2) were subjected to progressively increasing displacement cycles, after application of a constant axial load. Three fully reversed cycles were applied in each drift level. The intermediate cycles were applied at a magnitude of 1/3 of the preceding major drift levels, and testing continued until specimens lost more than 80% of their peak strength. CI-5 and CI-6 were subjected to the same cyclic loading protocol as of CI-2, except that displacement cycles were followed by a unidirectional push representative of the main shock in an earthquake that is preceded by some small cycles. However, the number of small cycles that a structure experiences before being imposed to the main shock is not known in advance and depends on many factors including the distance to the source, soil condition, and frequency content of the earthquake. Therefore, CI-6 was subjected to fewer cycles before the final unidirectional push as opposed to CI-5.

During collapse-level earthquake excitation, columns in an actual building will experience unsymmetrical displacement reversals with drift ratios progressively increasing in one direction until the structure fails. Therefore, symmetric cyclic loading protocols are probably not representative of collapse-level response. A near-collapse loading protocol (Loading Protocol 1) was developed based on results from extensive nonlinear time-history analyses of mid- to high-rise prototype buildings subjected to a suite of far-field earthquake records, and it was applied to specimen CI-1.

The developed loading protocol features symmetric cycles in the early portion of the test, but these eventually undergo a large excursion to represent significant yielding and plastic

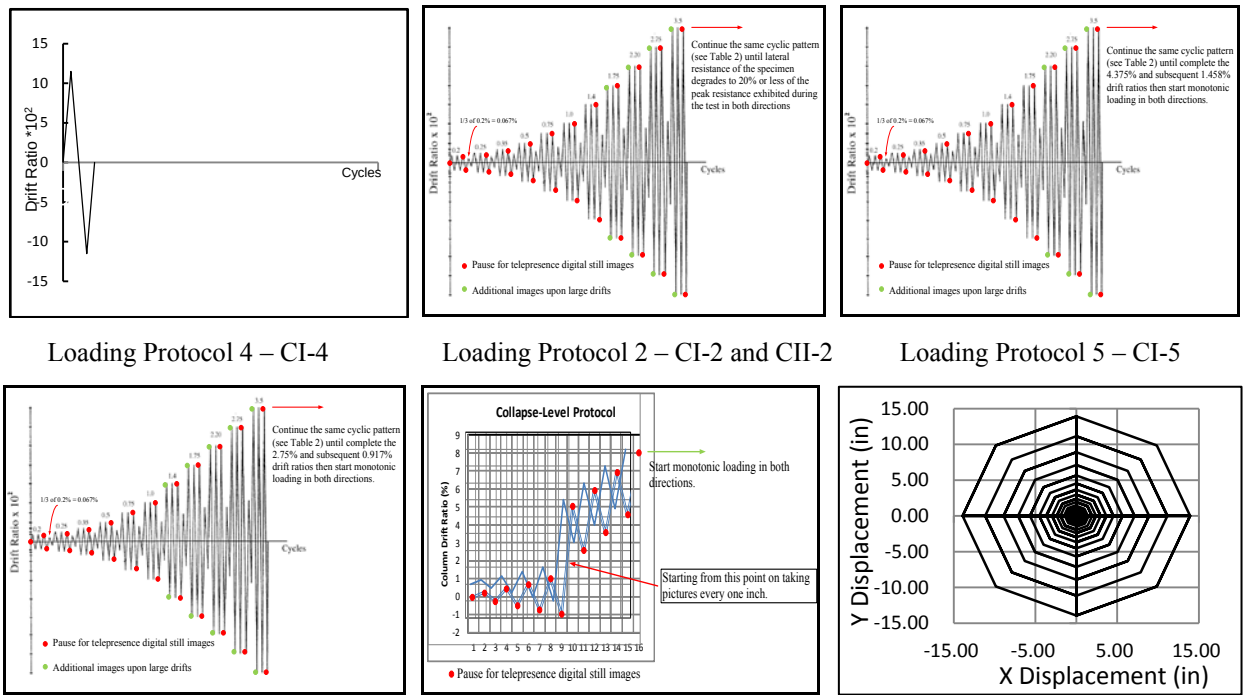

Loading Protocol 4 – CI-4 | Loading Protocol 2 – CI-2 and CII-2 | Loading Protocol 5 – CI-5

Loading Protocol 6 – CI-6 | Loading Protocol 1- CI-1 | Loading Protocol 7 – CI-7

Figure 2. Applied loading protocols and associate specimens.

deformation with permanent drift. The load cycles are continued at the offset drift, but the specimen is eventually loaded unidirectionally to represent a second excursion in which damage leads to collapse.

Although it is more convenient to idealize the lateral loading on a column uniaxially, all columns in practice will be exposed to biaxial loading protocols. Therefore, CI-7 was subjected to Loading Protocol 7 that features cyclic displacement reversals along its both axes as shown in Fig. 2. The cycles in each direction follow ACI 374-05 guidelines and they are designed such that an increase in drift ratios along one axis is always accompanied by a decrease along the other axis to make the results comparable with the other tests.

Test Observations

As the column specimens were subjected to lateral displacements, flexural cracks were observed on SE and NW faces of the columns as shown on Fig. 3. The first flexural crack was observed at about 12 in. from the column base at nearly 0.2% drift level (0.25 in. of crosshead displacement). On SW and NE faces, shear-flexural cracks were observed and expanded through the lower portion of the columns. Also, longitudinal cracks were observed adjacent to the compression sides. Yielding of the longitudinal reinforcements started at about 0.5% drift (0.65 in. of crosshead displacement). However, the applied lateral load still increased due to the resistance mobilized by the confining pressure of the transverse reinforcement and strain hardening of longitudinal reinforcement. As the applied lateral load reached the maximum

Figure 3. Progression of damage on CII-2: SW face at 3.5% drift (left), NW face at 3.5% drift (middle), and NW face at the end of the test (right).

capacity of the specimens, cracking, and progression of damage continued. The specimens started to lose flexural resistance due to crushing of the concrete along the perimeter of the column, and more significant degradation in strength when the buckling of the longitudinal reinforcement occurred. The sudden drop at large cycles (Fig. 4) resulted from fracture of the longitudinal bars. At the end of the tests, most of the longitudinal bars were fractured and severe damage around the core concrete in all specimens was observed. Also, some of the column ties were opened up due to the loss of cover and the lateral pressure of the buckled longitudinal bars.

As shown in Fig. 4, CI-2 exhibited lower displacement capacity before failure compared to CI-4 due to the effect of cyclic loading. The effect of number of preceding cycles on strength loss can also be observed by comparing cyclic envelopes of CI-5 and CI-6 in Fig. 5. As shown in Fig. 5, CI-5 degraded faster after reaching peak strength compared to CI-6 which underwent fewer displacement cycles. Also, compared to CI-4, progression of damage and spalling of the cover concrete occurred at lower drift levels in specimens subjected to cyclic loading (CI-1, CI-2, CI-5, CI-6, CI-7, and CII-2).

The effect of axial load ratio can be observed by comparing specimens CI-2, and CII-2. As shown in Figs. 4 and 5, when the applied lateral load reaches the maximum capacity of CII-2, large flexural moments at the base were introduced due to the high axial load ratio. The large second-order axial load effects (i.e., P-Delta effects) cause a faster rate of damage progression and lower displacement capacity in specimen CII-2.

Fig. 5 also illustrates the effect of biaxial loading protocol on the behavior of the specimen CI-7. As observed in Fig. 5, CI-7 exhibits a lower peak lateral load capacity, and drift ratio and faster damage progression and degradation compared to all other perimeter frame specimens due to the effect of applied displacement cycles in both directions.

Cyclic Envelopes

The cyclic load-deflection envelopes for the column specimens are shown in Fig. 5. These envelopes were obtained by connecting the peak applied lateral loads at the first cycle of each drift level. The envelopes shown in Fig. 5(b) can be represented in either loading direction as a

trilinear curve as shown in Fig. 5(c). The idealized envelope curve has an initial branch (from O to Y), a plastic branch (Y to P), and a degradation branch (P to U). For each of the cyclic envelope curves, the breakpoints (Y, P, and U) were identified graphically as the points of marked departure from linear elastic behavior (Y), end of the plastic region of the post-yield behavior (P), and end of the test (U), respectively. The stiffness (i.e., slope) in each of these branches was computed and normalized by the initial stiffness (i.e., slope of OY), and are given in Table 2. These values along with Fig. 5 indicate that among all specimens CII-2, which is under large axial load ratio, and CI-7, which is subjected to biaxial loading protocol, reached their ultimate breakpoints (U) much earlier than the other specimens. In these two specimens, displacement at the ultimate breakpoint (D_U) occurred at 7.1 in., which is smaller than that of the rest of the specimens. Also, CI-2 reached its ultimate displacement (D_U) of 8.9 in. that represents the deteriorating effect of the number of cycles. Moreover, the degradation slopes (K_u) of specimens CI-1 and CI-6 are much larger than that of CI-2. Specimens CI-1 and CI-6 undergo a small number of cycles followed by a large unidirectional displacement cycle that results in a huge strength loss in those specimens whereas in CI-2, smoothly increasing drift levels causes an earlier but smoother softening behavior. The last column in Table 2 represents the displacement ductility (μ_Δ) for each column specimen which is defined as the ratio of the displacement corresponding to 80% of the peak strength to the yield displacement (D_Y), and is averaged for the positive and negative loading directions. It is observed that increasing the number of load cycles results in a lower displacement ductility (CI-2 as opposed to CI-4).

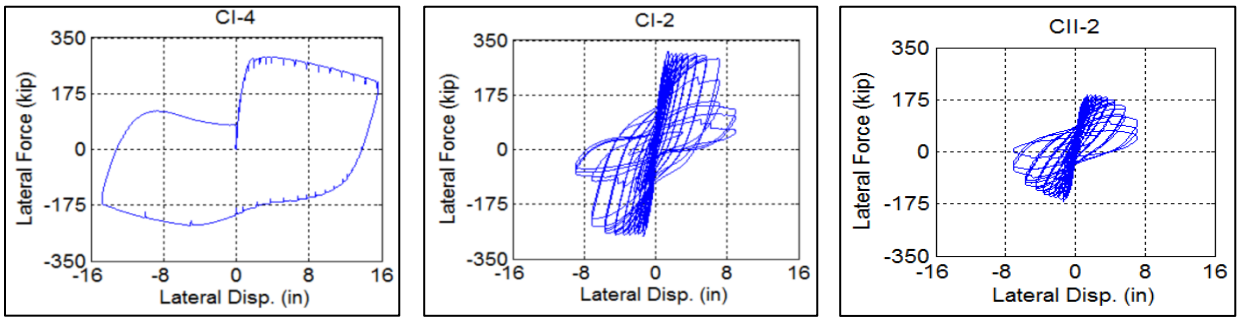

(a) (b) (c)

Figure 4. Lateral load vs. displacement relationship for columns: (a) CI-1; (b) CI-2; (c) CII-2.

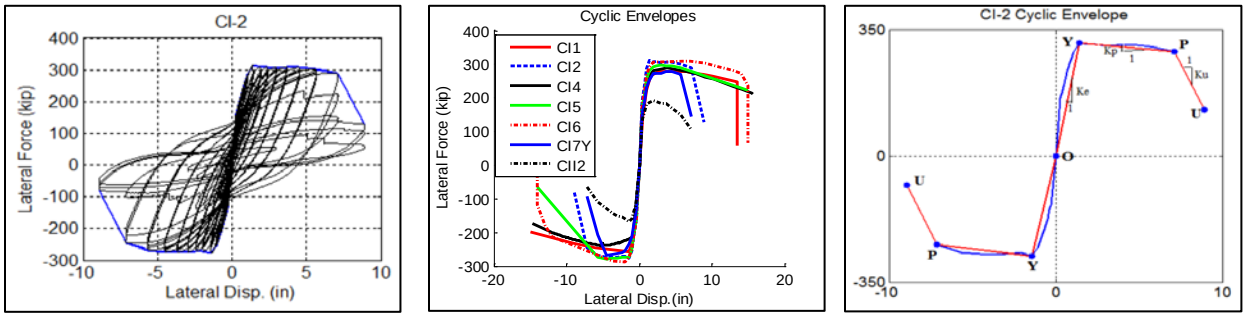

(a) (b) (c)

Figure 5. Load-deflection cyclic envelopes: (a) Generation based on cyclic response; (b) Cyclic envelopes for all specimens; (c) Trilinear approximation

Table 2. Characteristics of the cyclic envelopes.

Sp.	Peak		Trilinear Approximation									
	F *(kips)*	D *(in)*	F_Y *(kips)*	F_P *(kips)*	F_U *(kips)*	D_Y *(in)*	D_P *(in)*	D_U *(in)*	K_e *(kip/in)*	K_P/K_e *×100%*	K_u/K_e *×100%*	μ_Δ
CI-1	280.0	4.44	254.6	249.4	57.5	1.4	13.4	13.4	180.3	-0.24	-inf.	9.6
	-257.4	-1.41	-257.4	-245.3	-197.8	-1.4	-6.0	-15.0	182.7	-1.45	-2.89	
CI-2	313.9	1.39	313.0	289.6	128.4	1.4	7.1	8.9	222.0	-1.84	-40.77	5.3
	-277.6	-1.40	-277.6	-245.5	-80.7	-1.4	-7.1	-8.9	198.2	-2.83	-46.61	
CI-4	290.0	4.00	261.5	288.7	211.8	1.3	3.9	15.6	203.6	5.18	-3.22	10.2
	-239.5	-5.15	-217.6	-236.9	-172.3	-1.3	-4.7	-14.7	169.4	3.31	-3.81	
CI-5	296.8	2.97	282.4	295.2	221.9	1.4	4.5	15.0	201.9	2.02	-3.46	7.3
	-278.0	-4.52	-273.2	-273.4	-64.4	-1.4	-5.7	-14.0	195.3	0.02	-12.86	
CI-6	310.3	6.11	292.0	274.3	66.5	1.4	14.0	15.0	208.9	-0.67	-99.66	8.8
	-287.7	-1.95	-272.8	-212.5	-24.9	-1.4	-12.0	-14.0	193.2	-2.95	-48.59	
CI-7	279.1	4.54	253.5	270.4	145.4	1.4	5.7	7.1	180.1	2.21	-47.53	4.8
	-267.7	-4.54	-212.2	-267.7	-93.1	-1.1	-4.5	-7.1	198.1	8.09	-34.00	
CII-2	192.2	1.95	180.1	182.6	104.9	1.1	3.7	7.1	168.2	0.58	-13.29	4.5
	-168.4	-1.40	-158.2	-150.3	-65.1	-1.1	-3.0	-7.1	147.5	-2.80	-13.97	

Summary and Conclusions

Results of seven full-scale RC moment frame column tests were presented and discussed. To address the shortcomings in the available test data for rectangular RC columns, the specimens featured two different cross sectional dimensions that are larger than almost all columns tested before. Also, the specimens were subjected to a monotonic and several cyclic loading protocols that were continued to very large drift ratios (approaching 10%) and under which columns showed significant strength loss and softening behavior. The effect of loading history was investigated by comparing the load-displacement curves and cyclic envelopes of the test specimens. It was observed that columns exhibited faster strength degradation and stiffness deterioration under larger axial load, and larger number of preceding displacement cycles. It was also observed that biaxial loading results in a lower lateral load and displacement capacity. Furthermore, the load-deflection cyclic envelope for each test was approximated by a trilinear curve and similar results were obtained by comparing the breakpoints and slope of each branch on the trilinear curve. The location of the ultimate breakpoint and degradation slope on this curve were observed to be affected by axial load ratio, and properties of loading protocols.

Acknowledgement

This research was supported by the U.S. National Science Foundation (NSF) under award number CMMI-1041633. The authors acknowledge Mr. John D. Hooper of Magnusson Klemencic Associates, Professor Gregory Deierlein and the late Professor Helmut Krawinkler of Stanford University for their advice and guidance. Also, the assistance of the staff at the MAST lab of the University of Minnesota is gratefully appreciated.

References

[1] Advisory Committee on Earthquake Hazards Reduction (ACEHR). Effectiveness of the National Earthquake Hazards Reduction Program, *A Report from the Advisory Committee on earthquake Hazards Reduction*, 2008.

[2] National Institute of Standards and Technology (NIST). Research Required to Support Full Implementation of Performance-Based Seismic Design. NIST GCR 09-917-2, National Institute of Standards and Technology Building and Fire Research Laboratory, Gaithersburg, Maryland, 2009.
[3] Federal Emergency Management Agency (FEMA). Recommended Methodology for Quantification of Building System Performance and Response Parameters, FEMA P695, Prepared for the Federal Emergency Management Agency, Prepared by the Applied Technology Council, Redwood City, CA, 2009.
[4] Hart GC, Delli Quadri, NG. A Great Day and Why We Love ATC-63. *The Structural Design of Tall and Special Buildings* 2008; 17: 1015-1023.
[5] Berry M, Parrish M, Eberhard M. *PEER Structural Performance Database User's Manual, Pacific Engineering Research Center*, University of California, Berkeley, CA, 2004. Available at http://nisee.berkeley.edu/spd/ and http://maximus.ce.washington.edu/~peera1/.
[6] Bae S, Bayrak O. Seismic Performance of Full-Scale Reinforced Concrete Columns. *ACI Structural Journal* 2008; 105 (2): 123-132.
[7] Cheung PC, Paulay T, Park R. New Zealand Tests on Full-Scale Reinforced Concrete of Beam-Column-Slab Subassemblages Designed for Earthquake Resistance. *Design of Beam-Column Joints for Seismic Resistance*, Edited by J. O. Jirsa, SP-123, American Concrete Institute, Farmington Hills, MI, 1991.
[8] Kaku T, Asakusa H. Ductility estimation of exterior beam-column subassemblages in reinforced concrete frames. Design of beam-column joints for seismic resistance. American Concrete Institute, Farmington Hills, Mich., 1991: 167-185.
[9] Federal Emergency Management Agency (FEMA). Effects of Strength and Stiffness Degradation of Seismic Response, FEMA P440A, Prepared by the Applied Technology Council (Project ATC-62), Redwood City, CA, 2009.
[10] Haselton CB, Liel AB, Taylor Lange S, Deierlein GG. Beam-Column Element Model Calibrated for Predicting Flexural Response Leading to Global Collapse of RC Frame Buildings, *PEER Report 2007/03*, Pacific Engineering Research Center, University of California, Berkeley, CA, 2008.
[11] Dhakal RP, Fenwick RC. Detailing of Plastic Hinges in Seismic Design of Concrete Structures. *ACI Structural Journal 2008*; 105(6).
[12] Ingham JM, Lidell D, Davidson BJ. Influence of Loading History on the Response of a Reinforced Concrete Beam. *Bulletin of the New Zealand Society for Earthquake Engineering* 2001; (34)2: 107-124.
[13] Stone WC, Cheok GS, Stanton JF. Performance of Hybrid Moment-Resisting Precast Beam-Column Concrete Connections Subjected to Cyclic Loading. *ACI Structural Journal* 1995; 91(2): 229-249.
[14] Takemura H, Kawashima K. Effect of Loading Hysteresis on Ductility Capacity of Reinforced Concrete Bridge Piers. *Journal of Structural Engineering*, *Japan*,1997; 43A: 849- 858.
[15] Lehman DE, Moehle JP. Influence of Longitudinal Reinforcement Ratio on Column Response. Pacific Earthquake Engineering Research Center, University of California, Berkeley, CA, 1998.
[16] Jaradat OA, McLean DI, Marsh ML. Performance of Existing Bridge Columns Under Cyclic Loading- Part1: Experimental Results and Observed Behavior. *ACI Structural Journal* 1998; 95-S63: 695-704.
[17] Esmaeily-Gh A, Yan X. Seismic Behavior of Bridge Columns Subjected to Various Loading Patterns. *PEER Report 2002/15*, Pacific Engineering Research Center, University of California, Berkeley, CA, 2002.
[18] Gilbersten ND, Moehle JP. Experimental Study of Small-Scale R/C Columns Subjected to Axial and Shear Force Reversal. Structural Research Series No. 481, Civil Engineering Studies, University of Illinois, Urbana, 1980.
[19] Kreger ME, Linbeck L. Behavior of Reinforced Concrete Columns Subjected to Lateral and Axial Load Reversals. *Proceeding of the third U.S. National Conference on Earthquake Engineering*, Charleston, S.C., 1986.
[20] French CW, Schultz AE, Hajjar JF, Shield CK, Ernie DW, Dexter RJ, Du DHC, Olson SA, Daugherty DJ, Wan CP. Multi-Axial Subassemblage Testing (MAST) System: Description And Capabilities. Paper No. 2146, Proceedings of the 13th World Conference on Earthquake Engineering, Vancouver, BC, Canada, August 1-6, 2004.
[21] ACI Committee 318. Building Code Requirements for Reinforced Concrete and Commentary (ACI 318-11/ACI 318R-11). American Concrete Institute, Detroit, Michigan, 2011.
[22] ASTM International. Standard Test Methods and Definitions for Mechanical Testing of Steel Products. ASTM A 370-03a, 2003.
[23] ASTM International. Standard Test Method for Compressive Strength of Cylindrical Concrete Specimens. ASTM C 39C/C 39M, 2003.